Two-photon decay rates in heliumlike ions: Finite-nuclear-mass effects

Aaron T. Bondy,[1] Donald C. Morton,[2] and G. W. F. Drake[1]
[1]Department of Physics, University of Windsor, Windsor, Ontario, Canada N9B 3P4
[2]Herzberg Astronomy and Astrophysics, National Research Council, Victoria, British Columbia, Canada V9E 2E7

(Received 22 September 2020; accepted 21 October 2020; published 10 November 2020)

The spontaneous two-photon decay rates from the $1s2s\ ^1S_0$ level to the ground state $1s^2\ ^1S_0$ in helium and its isoelectronic ions through neon ($Z = 10$) are calculated, including the effects of finite nuclear mass. In all cases the length and velocity results agree to eight or more figures, demonstrating that the theoretical formulation correctly takes into account the effects of mass scaling, mass polarization, and motion of the nucleus in the center-of-mass frame. Algebraic relationships are derived and tested relating the expansion coefficients in powers of μ/M for mass polarization, where μ is the electron reduced mass and M is the nuclear mass. Muonic, pionic, and antiprotonic helium are included as extreme test cases where mass polarization is large. The results are compared with experiment and previous calculations.

DOI: 10.1103/PhysRevA.102.052807

I. INTRODUCTION

Two-photon processes have played an important role in many branches of physics ever since their first theoretical discussion by Goeppert-Mayer [1] as a second-order interaction between atoms and the electromagnetic field. The hallmark of two-photon transitions is that the two frequencies ω_1 and ω_2 form a broad continuum such that the energy conserving condition

$$\hbar\omega_1 + \hbar\omega_2 = E_\mathrm{i} - E_\mathrm{f} \tag{1}$$

is satisfied, where E_i and E_f are the energies of the initial and final states. In emission, two-photon decay determines the radiative lifetimes of metastable states such as $2\,^2S_{1/2}$ of hydrogen and $2\ ^1S_0$ of helium since the usual single-photon electric dipole ($E1$) transition to the ground state is forbidden by angular momentum and parity selection rules. Their long radiative lifetimes, together with collision rates, determine their population balance in astrophysical sources such as planetary nebulae [2]. They also largely determine the rate of radiation loss in the early universe to form the cosmological microwave background (CMB) since there is no resonant reabsorption of radiation [3,4]. In absorption, two-photon transitions can be driven by strong laser fields, giving rise to a wide variety of phenomena and a vast range of technological applications.

Following the initial theoretical analysis by Goeppert-Mayer, Breit and Teller [5] performed the first quantitative calculations for hydrogen $2\,^2S_{1/2}$-$1\,^2S_{1/2}$ and gave qualitative estimates for helium $2\ ^1S_0$ -$1\ ^1S_0$. More quantitative estimates were obtained by Dalgarno [6] from oscillator strength sum rules, and the first accurate calculations were performed by Drake *et al.* [7] for helium and the heliumlike ions up to Ne^{8+}. These calculations demonstrated the approximate Z^6 scaling of the decay rates from 51.3 s^{-1} for He to $1.00 \times 10^7\ \mathrm{s}^{-1}$ for Ne^{8+}. The accuracy was further improved by Drake [8], including an estimate of relativistic corrections derived from the one-electron case [9], and extended to all ions up to U^{90+}. The first fully relativistic calculations were performed by Derevianko and Johnson [10], using a relativistic configuration-interaction method, and found to be in good agreement with Ref. [8]. They also confirmed previous investigations [7,11] that the triplet-to-singlet decay rates are negligible at low atomic number, with the ratio increasing from 6.2×10^{-11} at $Z = 2$ to 2.6×10^{-6} at $Z = 16$.

On the experimental side, measurements of the total decay rate have been made for He [12], and the six He-like ions with $Z = 3$, 18, 28, 35, 36, and 41 [13–18], as reviewed by Mokler and Dunford [19]. Recent work has focused on the photon spectral distribution functions for heavy-heliumlike ions up to $Z = 92$ using relativistic Green's function methods [20] in comparison with experiment [21]. For the corresponding hydrogenic case, the angular and polarization dependence of the photons in the relativistic region has been studied by Safari *et al.* [22], including the hyperfine structure.

Although the general theory of two-photon processes is well established within the framework of quantum electrodynamics (QED) [23], past calculations have been carried out almost exclusively within the approximation of infinite nuclear mass. The main focus of the present work is to investigate in detail the effects of finite nuclear mass on two-photon processes, taking high-precision calculations for the $1\ ^1S_0$ and $2\ ^1S_0$ states of helium and the heliumlike ions up to Ne^{8+} as an illustrative example. As will be shown, the effects of mass scaling and mass polarization must be taken into account, along with radiation due to the motion of the nucleus in the center-of-mass frame, in order to obtain agreement between the well-known "length" (L) and "velocity" (V) forms of the interaction. As a consequence, there are interesting algebraic relationships among the various contributions, as will be derived and verified numerically in the present work. They provide a more sensitive way of testing the equivalence of the length and velocity formulations than a direct comparison of the total two-photon decay rates themselves. They also facilitate the calculation of two-photon decay rates for other isotopes, or for an adjusted value of the atomic mass.

In related work, Barton and Calogeracos [24] considered the general question of transition rates in atoms constrained to move with relativistic velocities. For the case of uniform nuclear motion, they showed that the only correction is the normally expected one from relativistic time dilation, in contradiction to an earlier suggestion in Ref. [25] that there may be an additional scalar photon interaction due to finite-mass corrections.

In the balance of this paper, we first review in Sec. II the case of finite-mass corrections for single-photon transitions, as derived from Fermi's golden rule, and then generalize to the case of two-photon transitions by a direct extension of Fermi's golden rule. In Sec. III we briefly review the doubled Hylleraas wave functions used in the calculations, and then derive algebraic expressions relating the expansion coefficients for the L and V forms of the two-photon decay rates in powers of μ/M, where μ is the electron reduced mass and M is the nuclear mass. The results in Sec. IV demonstrate that the V form of the two-photon decay rate has converged to 5 parts in 10^9, and the L form to 2 parts in 10^8 for helium. The results also verify our derived algebraic relationships relating the expansion coefficients in powers of μ/M. As test cases where μ/M is not small, we present results for heavy-helium atoms where both electrons are replaced by muons (μ^2-He), pions (π^2-He), and antiprotons ($\bar{\mathrm{p}}^2$-He). The results verify that the theoretical formulation for the finite-mass corrections is correct, including mass scaling, mass polarization, and motion of the nucleus in the center-of-mass (c.m.) frame. Section V provides a brief discussion of astrophysical applications, and Sec. VI some further discussion and conclusions.

II. THEORY

For helium and the lighter heliumlike ions, the appropriate starting point for a discussion of finite-nuclear-mass effects is the Schrödinger equation in an inertial coordinate system. For an atom with atomic number Z and nuclear mass M located at $\mathbf{R}_\mathrm{N}$ and N electrons of mass m_e located at $\mathbf{R}_i$, the nonrelativistic Hamiltonian is

$$H_\mathrm{inert} = \frac{\mathbf{P}_\mathrm{N}^2}{2M} + \sum_{i=1}^{N}\left(\frac{\mathbf{P}_i^2}{2m_\mathrm{e}} - \frac{Ze^2/4\pi\epsilon_0}{|\mathbf{R}_i - \mathbf{R}_N|} + \sum_{j>i}^{N}\frac{Ze^2/4\pi\epsilon_0}{|\mathbf{R}_j - \mathbf{R}_i|}\right) \tag{2}$$

in SI units [26], where $\mathbf{P} = -i\hbar\nabla_\mathrm{R}$. The Schrödinger equation

$$H_\mathrm{inert}|u\rangle = E_u|u\rangle \tag{3}$$

then determines the energy levels E_u and eigenvectors $|u\rangle$. To simplify the solution, the usual procedure is to transform to center-of-mass (c.m.) plus relative coordinates defined by

$$\mathbf{R}_\mathrm{c.m.} = \frac{M\mathbf{R}_\mathrm{N} + m_\mathrm{e}\sum\mathbf{R}_i}{M + Nm_\mathrm{e}}, \tag{4}$$

$$\mathbf{r}_i = \mathbf{R}_i - \mathbf{R}_\mathrm{N}. \tag{5}$$

Transforming (2) to coordinates $\mathbf{r}_i = \mathbf{R}_i - \mathbf{R}_\mathrm{N}$ and $\mathbf{R}_\mathrm{c.m.} = \mathbf{0}$ so that

$$(M + Nm_\mathrm{e})\mathbf{R}_\mathrm{N} + m_\mathrm{e}\sum_{i=1}^{N}\mathbf{r}_i = \mathbf{0} \tag{6}$$

and taking the conserved total momentum to be zero in the absence of external forces resulting in

$$\sum_{i=1}^{N}\mathbf{P}_i = \sum_{i=1}^{N}\mathbf{p}_i \quad \text{and} \quad \mathbf{P}_\mathrm{N} + \sum_{i=1}^{N}\mathbf{p}_i = \mathbf{0} \tag{7}$$

gives

$$H_\mathrm{c.m.} = \frac{1}{2\mu}\sum_{i=1}^{N}\mathbf{p}_i^2 + \frac{1}{M}\sum_{i=1}^{N}\sum_{j>i}^{N}\mathbf{p}_i\cdot\mathbf{p}_j + \frac{1}{2(M+Nm_\mathrm{e})}\mathbf{P}_\mathrm{c.m.}^2 - \sum_{i=1}^{N}\left(\frac{Ze^2/4\pi\epsilon_0}{|\mathbf{r}_i|} + \sum_{j>i}^{N}\frac{Ze^2/4\pi\epsilon_0}{|\mathbf{r}_j - \mathbf{r}_i|}\right). \tag{8}$$

Here, μ is the reduced electron mass $\mu = m_\mathrm{e}M/(m_\mathrm{e} + M)$, the term $\sum_{j>i}\mathbf{p}_i\cdot\mathbf{p}_j/M$ is the mass-polarization operator, and the term involving $\mathbf{P}_\mathrm{c.m.} = -i\hbar\nabla_{R_\mathrm{c.m.}}$ accounts for the motion of the center of mass relative to the inertial frame represented by the coordinates $\mathbf{R}_\mathrm{N}$ and $\mathbf{R}_i$.

We next include the interaction with the radiation field, specified by its vector potential

$$\mathbf{A}(\mathbf{R},t) = A_0(\omega)\hat{\boldsymbol{\epsilon}}\,e^{i\mathbf{k}\cdot\mathbf{R}-i\omega t} + \text{c.c.}, \tag{9}$$

where

$$A_0(\omega) = c\left(\frac{\hbar}{2\epsilon_o\omega\mathcal{V}}\right)^{1/2} \tag{10}$$

for a photon of frequency ω, wave vector $\mathbf{k}$ ($|\mathbf{k}| = \omega/c$), and polarization $\hat{\boldsymbol{\epsilon}} \perp \mathbf{k}$. The factor $A_0(\omega)$ normalizes the vector potential to unit photon energy $\hbar\omega$ in volume $\mathcal{V}$. In a semiclassical picture, the interaction Hamiltonian with the radiation field is obtained by making the minimal coupling replacements

$$\mathbf{P}_\mathrm{N} \to \mathbf{P}_\mathrm{N} - Ze\mathbf{A}(\mathbf{R}_\mathrm{N}), \tag{11}$$

$$\mathbf{P}_i \to \mathbf{P}_i + e\mathbf{A}(\mathbf{R}_i), \tag{12}$$

for the canonical momenta in the inertial Hamiltonian H_inert in (2). The linear coupling terms then yield

$$H_\mathrm{int} = -\frac{Ze}{Mc}\mathbf{P}_\mathrm{N}\cdot\mathbf{A}(\mathbf{R}_\mathrm{N}) + \frac{e}{m_\mathrm{e}c}\sum_{i=1}^{N}\mathbf{P}_i\cdot\mathbf{A}(\mathbf{R}_i). \tag{13}$$

A. Single-photon transitions

As a point of reference, we first briefly review the well-known case of single-photon transitions for a finite nuclear mass, as first discussed by Fried and Martin [27], and extended by Yan and Drake [28] and Drake and Morton [29]. From Fermi's golden rule, the decay rate for spontaneous emission from state i to f is

$$w_\mathrm{i,f}d\Omega = \frac{2\pi}{\hbar}|\langle\mathrm{i}|H_\mathrm{int}|\mathrm{f}\rangle|^2\rho(\omega)d\Omega, \tag{14}$$

where

$$\rho(\omega) = \frac{\mathcal{V}\omega^2}{(2\pi c)^3\hbar} \tag{15}$$

is the number of photon states with polarization $\hat{\boldsymbol{\epsilon}}$ per unit energy in the normalization volume $\mathcal{V}$. In the long-wavelength and electric dipole approximations, the factor $e^{i\mathbf{k}\cdot\mathbf{R}}$ in Eq. (9) is replaced by unity. After integrating over angles $d\Omega$ and summing over polarizations $\hat{\boldsymbol{\epsilon}}$, the decay rate reduces to the familiar expression [30] (see Appendix)

$$w_{\rm i,f} = \tfrac{4}{3}\alpha\omega_{\rm i,f}|\langle{\rm i}|\mathbf{Q}_P|{\rm f}\rangle|^2, \tag{16}$$

where $\omega_{\rm i,f}$ is the transition frequency and, as follows from Eq. (13), $\mathbf{Q}_P$ is the dimensionless velocity form of the transition operator

$$\mathbf{Q}_P = -\frac{Z}{Mc}\mathbf{P}_{\rm N} + \frac{1}{m_{\rm e}c}\sum_{i=1}^{N}\mathbf{P}_i \tag{17}$$

for the general case of N electrons. From the commutator

$$[H_{\rm inert}, \mathbf{Q}_R/\hbar\omega_{\rm i,f}] = \mathbf{Q}_P, \tag{18}$$

where $H_{\rm inert}$ is the field-free Hamiltonian in Eq. (2), the equivalent length form is

$$\mathbf{Q}_R = -\frac{i}{c}\omega_{\rm i,f}\left(Z\mathbf{R}_{\rm N} - \sum_{i=1}^{N}\mathbf{R}_i\right), \tag{19}$$

all expressed in the inertial frame.

Transforming now to c.m. plus relative coordinates, the dipole transition operators become

$$\mathbf{Q}_p = \frac{Z_p}{m_{\rm e}c}\sum_{i=1}^{N}\mathbf{p}_i, \quad \mathbf{Q}_r = \frac{i\omega_{\rm i,f}}{c}Z_r\sum_{i=1}^{N}\mathbf{r}_i, \tag{20}$$

with

$$Z_p = \frac{Zm_{\rm e}+M}{M}, \quad Z_r = \frac{Zm_{\rm e}+M}{Nm_{\rm e}+M},$$

and $H_{\rm c.m.}$ now contains the mass-polarization term. These definitions are consistent with the commutation relation

$$[H_{\rm c.m.}, \mathbf{Q}_r] = \hbar\omega\mathbf{Q}_p. \tag{21}$$

If Eq. (3) is solved exactly for the states $|{\rm i}\rangle$ and $|{\rm f}\rangle$, then the identity

$$\langle{\rm i}|\mathbf{Q}_p|{\rm f}\rangle = \langle{\rm i}|\mathbf{Q}_r|{\rm f}\rangle \tag{22}$$

is satisfied to all orders in $m_{\rm e}/M$. For a neutral atom, $N = Z$ and $Z_r = 1$. If, following Ref. [29], the oscillator strength is defined by

$$f_{\rm i,f} = \frac{2m_{\rm e}c^2}{3\hbar\omega_{\rm i,f}}\langle{\rm i}|\mathbf{Q}_p\cdot\hat{\boldsymbol{\epsilon}}|{\rm f}\rangle\langle{\rm f}|\mathbf{Q}_r\cdot\hat{\boldsymbol{\epsilon}}|{\rm i}\rangle, \tag{23}$$

then the Thomas-Reiche-Kuhn sum rule $\sum_{\rm f} f_{\rm i,f} = N$ is modified to read [29]

$$\sum_{\rm f} f_{\rm i,f} = N + Z^2m_{\rm e}/M \tag{24}$$

with emission counted as negative and absorption as positive. In this way, the sum is 2 for positronium (Ps), but 3 for Ps^-, as expected for two or three radiating particles of the same mass. The above formulas provide a smooth interpolation between the two extremes. An advantage of this definition is that the decay rate, summed over final states and averaged over initial states, has the conventional form

$$\bar{w}_{\rm i,f} = -\frac{2\alpha\hbar\omega_{\rm i,f}^2}{m_{\rm e}c^2}\bar{f}_{\rm i,f}, \tag{25}$$

where $\bar{f}_{\rm i,f} = -(g_{\rm f}/g_{\rm i})\bar{f}_{\rm f,i}$ is the (negative) oscillator strength for photon emission from state $|{\rm i}\rangle$, and $g_{\rm i}$, $g_{\rm f}$ are the statistical weights of the states.

B. Two-photon transitions

The triply differential rate for the simultaneous emission of two photons of frequencies ω_1 and ω_2 can similarly be expressed via Fermi's golden rule in the form

$$dw^{(2\gamma)}d\Omega_1\,d\Omega_2 = \frac{2\pi}{\hbar}\left|U_{\rm i,f}^{(2)}\right|^2\rho(\omega_1)\rho(\omega_2)d\Omega_1\,d\Omega_2\,dE_1, \tag{26}$$

where, in a nonrelativistic approximation, $U_{\rm i,f}^{(2)}$ is a second-order interaction energy with the electromagnetic field given by

$$U_{\rm i,f}^{(2)} = -\sum_n\left[\frac{\langle{\rm f}|H_{\rm int}(\omega_1)|n\rangle\langle n|H_{\rm int}(\omega_2)|{\rm i}\rangle}{E_n - E_{\rm i} + \hbar\omega_2} + \frac{\langle{\rm f}|H_{\rm int}(\omega_2)|n\rangle\langle n|H_{\rm int}(\omega_1)|{\rm i}\rangle}{E_n - E_{\rm i} + \hbar\omega_1}\right] \tag{27}$$

summed over positive energy states, and by conservation of energy

$$E_{\rm i} - E_{\rm f} = \hbar\omega_1 + \hbar\omega_2. \tag{28}$$

This leads to a broad distribution of photon energies such that their sum is equal to the atomic energy difference. Using Eqs. (15) and (10) for $\rho(\omega)$ and A_0, and approximating $\mathbf{A} = A_0\hat{\boldsymbol{\epsilon}}$, the two-photon decay rate becomes

$$dw^{(2\gamma)}d\Omega_1\,d\Omega_2 = \frac{\alpha^2\hbar\omega_1\omega_2}{(2\pi)^3}\left|\sum_n\left[\frac{\langle{\rm f}|\mathbf{Q}_p\cdot\hat{\boldsymbol{\epsilon}}_1|n\rangle\langle n|\mathbf{Q}_p\cdot\hat{\boldsymbol{\epsilon}}_2|{\rm i}\rangle}{E_n - E_{\rm i} + \hbar\omega_2} + \frac{\langle{\rm f}|\mathbf{Q}_p\cdot\hat{\boldsymbol{\epsilon}}_2|n\rangle\langle n|\mathbf{Q}_p\cdot\hat{\boldsymbol{\epsilon}}_1|{\rm i}\rangle}{E_n - E_{\rm i} + \hbar\omega_1}\right]\right|^2 d\Omega_1\,d\Omega_2\,dE_1. \tag{29}$$

This must still be summed over two linearly independent sets of polarization vectors $\hat{\boldsymbol{\epsilon}}_1$ and $\hat{\boldsymbol{\epsilon}}_2$, and integrated over angles. For S-S transitions via intermediate P states, the matrix elements squared are proportional to $|\hat{\boldsymbol{\epsilon}}_1\cdot\hat{\boldsymbol{\epsilon}}_2|^2$, and the sum over polarization vectors yields an angular correlation factor of $1 + \cos^2\theta_{12}$ (see Appendix). The remaining angular integral is

$$\int_{4\pi} d\Omega_1 \int_{4\pi} d\Omega_2(1 + \cos^2\theta_{12}) = \frac{64\pi^2}{3}. \tag{30}$$

The final result for singly differential decay rate for the case of the helium $2\ ^1S$ state is thus

$$\frac{dw^{(2\gamma)}}{d\omega_1} = \frac{8\alpha^2}{3\pi}|Q^{(2\gamma)}(\omega_1,\omega_2)|^2, \tag{31}$$

where the dimensionless quantity $Q^{(2\gamma)}$ can be expressed in either the velocity form (p),

$$Q_p^{(2\gamma)}(\omega_1,\omega_2) = -(\omega_1\omega_2)^{1/2}\sum_n \langle 1\ ^1S\,|Q_{p,z}|n\,^1P\rangle\langle n\,^1P|Q_{p,z}|2\ ^1S\rangle\left(\frac{1}{\omega_n-\omega_\mathrm{i}+\omega_2}+\frac{1}{\omega_n-\omega_\mathrm{i}+\omega_1}\right), \tag{32}$$

or, with the use of Eq. (22) together with sum rules [31], the length (r) form as

$$Q_r^{(2\gamma)}(\omega_1,\omega_2) = -(\omega_1\omega_2)^{1/2}\sum_n \langle 1\ ^1S\,|Q'_{r,z}|n\,^1P\rangle\langle n\,^1P|Q'_{r,z}|2\ ^1S\rangle\left(\frac{1}{\omega_n-\omega_\mathrm{i}+\omega_2}+\frac{1}{\omega_n-\omega_\mathrm{i}+\omega_1}\right), \tag{33}$$

where $\omega_\mathrm{i} = E_\mathrm{i}/\hbar$ and $Q_{p,z}$ and $Q'_{r,z}$ are the z components of the vectors $\mathbf{Q}_p$ and $\mathbf{Q}'_r$, and, in parallel with Eq. (20), are defined by

$$\mathbf{Q}_p = \frac{1}{m_\mathrm{e}c}Z_p\sum_{i=1}^{N}\mathbf{p}_i \tag{34}$$

and

$$\mathbf{Q}'_r = \frac{i(\omega_1\omega_2)^{1/2}}{c}Z_r\sum_{i=1}^{N}\mathbf{r}_i. \tag{35}$$

Note that the definition of $\mathbf{Q}'_r$ is slightly different from the corresponding $\mathbf{Q}_r$ in the single-photon case, but $\mathbf{Q}_p$ is the same. The equivalence of the velocity and length forms can also be regarded as a gauge transformation, as discussed in general by Goldman and Drake [9]. A numerical comparison of the two provides a check on the accuracy of the calculations since it is valid only if the wave functions are exact, and the sum over intermediate states is complete, as discussed in the following section. Finally, the integrated two-photon decay rate is

$$\begin{aligned} w^{(2\gamma)} &= \frac{1}{2}\int_0^\Delta \frac{dw^{(2\gamma)}}{d\omega_1}d\omega_1 \\ &= \frac{4\alpha^2\Delta}{3\pi}\int_0^1 |Q^{(2\gamma)}(y)|^2dy, \end{aligned} \tag{36}$$

where $y = \omega_1/\Delta$, $\Delta = (E_\mathrm{i}-E_\mathrm{f})/\hbar$, and the factor of 1/2 is included because each pair of photons should be counted only once.

III. CALCULATIONS

A. Wave functions

For purposes of calculations, it is convenient to transform to reduced-mass atomic units of distance, time, momentum, and energy, respectively defined by

$$\begin{aligned} \rho &= \frac{\mu}{m_\mathrm{e}}\frac{a_0}{\hbar}, \quad \tau = \frac{\mu}{m_\mathrm{e}}\frac{a_0}{\alpha c}t, \\ i\nabla &= -\frac{m_\mathrm{e}}{\mu}\frac{a_0}{\hbar}\mathbf{p}, \quad \epsilon = \left(\frac{m_\mathrm{e}}{\mu}\right)\frac{E}{\alpha^2 m_\mathrm{e}c^2}, \end{aligned} \tag{37}$$

so that the Schrödinger equation assumes the dimensionless form for two electrons (or other particles with mass m_x in place of m_e)

$$\left[-\frac{1}{2}(\nabla^2_{\rho_1}+\nabla^2_{\rho_2}) - \frac{\mu}{M}\nabla_{\rho_1}\cdot\nabla_{\rho_2} + V(\rho_1,\rho_2)\right]\Psi = \epsilon\Psi, \tag{38}$$

where

$$V(\rho_1,\rho_2) = -\frac{Z}{\rho_1}-\frac{Z}{\rho_2}+\frac{1}{|\rho_1-\rho_2|}.$$

The two-electron wave functions for the initial and final S states, and the intermediate P states are all calculated variationally in terms of correlated two-electron double basis sets of the form [32]

$$\Psi = c_0\Psi_0 + \sum_{ijk}^{i+j+k\leqslant\Omega}\left[\underbrace{c_{ijk}^{(\mathrm{A})}\varphi_{ijk}(\alpha_\mathrm{A},\beta_\mathrm{A})}_{\text{A sector}} + \underbrace{c_{ijk}^{(\mathrm{B})}\varphi_{ijk}(\alpha_\mathrm{B},\beta_\mathrm{B})}_{\text{B sector}}\right], \tag{39}$$

where Ψ_0 is the screened hydrogenic term and the basis functions $\varphi_{ijk}(\alpha,\beta)$ are defined by

$$\varphi_{ijk}(\alpha,\beta) = r_1^i\,r_2^j\,r_{12}^k\,e^{-\alpha r_1-\beta r_2}\,\mathcal{Y}^M_{l_1,l_2,L}(\hat{r}_1,\hat{r}_2) \pm \text{exchange} \tag{40}$$

in Hylleraas coordinates. In general, the quantity $\mathcal{Y}^M_{l_1,l_2,L}(\hat{r}_1,\hat{r}_2)$ represents a vector-coupled product of spherical harmonics of angular momenta l_1 and l_2 to form a state with total angular momentum L and component M. The parameter $\Omega = (i+j+k)_\mathrm{max}$ controls the size of the basis set. The nominal number of terms in each sector is

$$N = \tfrac{1}{6}(\Omega+1)(\Omega+2)(\Omega+3). \tag{41}$$

The basis set is "doubled" in the sense that different nonlinear parameters $\alpha_\mathrm{A},\beta_\mathrm{A}$ and $\alpha_\mathrm{B},\beta_\mathrm{B}$ are used for the asymptotic (A) and short-range (B) sectors, respectively. The nonlinear parameters are determined by calculating analytically the four derivatives $\partial E/\partial\alpha_X$ and $\partial E/\partial\beta_X$, and finding the zeros by Newton's method [33,34]. An advantage of these doubled basis sets is their compactness and numerical stability such that standard quadruple precision (approximately 32 decimal digits) in FORTRAN is sufficient, even for the largest basis sets with up to 1566 terms.

The sum over intermediate states, including an integration over the continuum, is performed by summing instead over the set of N discrete variational pseudostates obtained by diagonalizing the Hamiltonian in the same basis set as for the optimized 2^1P state such that

$$\langle\Psi_n|H|\Psi_m\rangle = \epsilon_n\delta_{n,m}, \quad \langle\Psi_n|\Psi_m\rangle = \delta_{n,m}. \tag{42}$$

The pseudostates represent a two-electron generalization of a Coulomb Sturmian basis set for hydrogen.

B. Finite nuclear mass

The effects of a finite nuclear mass come from three sources. The first is due to the radiation emitted by the nucleus as it moves in the c.m. frame. This is taken into account by factors of Z_p^4 and Z_r^4 in the velocity and length forms, respectively. The second, analogous to the normal isotope shift, is due to the mass scaling of the energies, transition frequencies, and matrix elements as calculated from wave functions expressed in reduced-mass atomic units according to Eq. (37). Since the Q' terms in Eqs. (34) and (35) occur with the fourth power in the integral (36) along with the frequency factor Δ, the factors to transform the reduced atomic units to physical ones are $(\mu/m_e)^5$ for $w_p^{(2\gamma)}$ and (μ/m_e) for $w_r^{(2\gamma)}$.

The third correction comes from the direct effect of the mass-polarization term $-\frac{\mu}{M}\nabla_{\rho_1}\cdot\nabla_{\rho_2}$ in Eq. (38) on the wave functions, energies, and matrix elements, analogous to the specific isotope shift. The result can be expressed as a correction factor $F(\mu/M)$ to the two-photon decay rate for infinite nuclear mass $w_\infty^{(2\gamma)}$. For small μ/M, it is useful to expand $F(\mu/M)$ in the form

$$F_x(\mu/M) = 1 + (\mu/M)C_x + (\mu/M)^2D_x + \cdots, \tag{43}$$

where C_x and D_x correspond to first- and second-order mass-polarization corrections, and $x = p$ or r since the coefficients are different for the V and L cases. For helium and the heliumlike ions, $\mu/M \sim 10^{-4}$, and so terms beyond D_x are negligible. The coefficients C_x and D_x could be calculated by perturbation theory, but we have adopted the simple expedient of calculating $F_x(\mu/M)$ for an arbitrary pair of values of μ/M and solving for C_x and D_x. The residual error of order $(\mu/M)^3$ is negligible. The final result for the two-photon decay rate from all three sources is

$$w_p^{(2\gamma)} = Z_p^4\left(\frac{\mu}{m_e}\right)^5F_p(\mu/M)w_{p,\infty}^{(2\gamma)}, \tag{44}$$

$$w_r^{(2\gamma)} = Z_r^4\left(\frac{\mu}{m_e}\right)F_r(\mu/M)w_{r,\infty}^{(2\gamma)}, \tag{45}$$

where $w_{x,\infty}^{(2\gamma)}$ is the corresponding two-photon decay rate for the case of infinite nuclear mass.

Since we must have $w_p^{(2\gamma)}/w_{p,\infty}^{(2\gamma)} = w_r^{(2\gamma)}/w_{r,\infty}^{(2\gamma)}$ if the wave functions contributing to each of the four rates are exact and the pseudostate expansions are complete, the coefficients must be equal term by term in the series expansion (43) in powers of μ/M. If we expand Z_p/Z_r in powers of m_e/M and approximate that ratio as $m_e/M \simeq \mu/M + (\mu/M)^2$, we find from the first and second powers of μ/M that the coefficients C_x and D_x for a two-electron atom or ion must satisfy

$$C_p - C_r = -4 \tag{46}$$

and

$$4C_p + D_p - D_r = -6. \tag{47}$$

A similar analysis of mass effects for single-photon emission with

$$w_p^{(1\gamma)} = Z_p^2\left(\frac{\mu}{m_e}\right)^3F_p(\mu/M)w_{p,\infty}^{(1\gamma)}, \tag{48}$$

$$w_r^{(1\gamma)} = Z_r^2\left(\frac{\mu}{m_e}\right)F_r(\mu/M)w_{r,\infty}^{(1\gamma)}. \tag{49}$$

gives velocity and length coefficients [35]

$$C_p - C_r = -2$$

and

$$2C_p + D_p - D_r = -1. \tag{50}$$

IV. NUMERICAL RESULTS

We have investigated 14 heliumlike systems. specifically ^{4}He and its isotope ^{3}He, ^{7}Li and its isotope ^{6}Li, and the most abundant forms for the rest of the isoelectronic sequence to ^{10}Ne. For all of these, μ/M is sufficiently small that a power-series expansion in powers of μ/M is useful, and so they provide an opportunity to check the algebraic relationships (46) and (47) relating the coefficients. In addition, we studied three heavy-helium species $\bar{\text{p}}^2$-^{4}He, π^2-^{4}He, and μ^2-^{4}He in which the two electrons are replaced by antiprotons, pions, and muons, respectively. Although these would be difficult to observe experimentally, the values of μ/M are so large ($0.2011\ldots$ for $\bar{\text{p}}^2$) that many terms contribute to the expansion in powers of μ/M, and so the comparison of the length and velocity forms provides a check that the mass dependence is correct to all orders in μ/M.

Table I shows as a typical example the convergence of the velocity and length rates with increasing Ω for ^{4}He. (The basis sets for $1\,^1S$ are a little larger than those for $2\,^1S$.) The rates are tabulated in atomic units and divided by α^6 so that the accuracies are not limited by the uncertainty in the fine-structure constant α. The velocity rates increase while the length rates decrease in larger steps to the same final value within 2 parts in 10^8 for $\Omega = 16$ and 1 part in 10^8 for the extrapolated values. This is typical for all the systems studied with slightly poorer convergence for larger μ/M and better for the more higher-Z ions reaching 6 parts in 10^9 for ^{20}Ne^{8+} with $\Omega = 16$, and 6 parts in 10^{10} for the extrapolated values, altogether providing confidence in the reliability of our wave functions. Consequently, we have quoted extrapolated velocity values in Tables II and III and used extrapolations for both velocity and length to obtain Table IV.

Table II compares the length and velocity forms for all 14 systems. It is clear that the length and velocity forms agree to within the convergence uncertainty of about one part in 10^8 or better over the entire range of μ/M, including the three heavy-helium species. The results verify that the combined mass dependence from all three sources—mass scaling, mass polarization, and nuclear motion—have been correctly calculated, and all three must be included to bring the L and V forms into agreement.

Next, to investigate the algebraic relations (46) and (47) for the mass-polarization coefficients, we estimated the coefficients by a method of finite differencing in which we extended the calculations to a third data set (in addition to $w_\infty^{(2\gamma)}$) with

TABLE I. Convergence with respect to basis set size (N) of the ^{4}He($2\,^1S_0$) two-photon decay rates $w_r^{(2\gamma)}/\alpha^6$ for a finite nuclear mass $\mu/M = 1.370\,745\,62 \times 10^{-4}$. The subscripts p and r denote the velocity (V) and length (L) forms, respectively. Units are atomic units. To convert to s^{-1}, multiply by $\alpha^6/\tau_e = 6242.763\,420(56)$ s^{-1} where $\alpha = 7.297\,352\,5693(11) \times 10^{-3}$ is the fine-structure constant and $\tau_e = 2.418\,884\,326\,5857(47) \times 10^{-17}$ s is the atomic unit of time.

Ω	$N(2\,^1S)$	$N(2\,^1P)$	$w_p^{(2\gamma)}/\alpha^6$	$w_r^{(2\gamma)}/\alpha^6$
4	44	104	$8.169\,161\,866\,046 \times 10^{-3}$	$8.182\,145\,206\,238 \times 10^{-3}$
5	67	145	$8.170\,301\,592\,330 \times 10^{-3}$	$8.174\,691\,464\,231 \times 10^{-3}$
6	98	197	$8.170\,633\,057\,717 \times 10^{-3}$	$8.171\,830\,051\,527 \times 10^{-3}$
7	135	265	$8.170\,667\,222\,361 \times 10^{-3}$	$8.171\,125\,033\,845 \times 10^{-3}$
8	182	346	$8.170\,684\,766\,627 \times 10^{-3}$	$8.170\,855\,798\,069 \times 10^{-3}$
9	236	446	$8.170\,690\,486\,882 \times 10^{-3}$	$8.170\,747\,017\,232 \times 10^{-3}$
10	301	559	$8.170\,691\,869\,889 \times 10^{-3}$	$8.170\,730\,900\,210 \times 10^{-3}$
11	373	692	$8.170\,692\,739\,038 \times 10^{-3}$	$8.170\,701\,468\,677 \times 10^{-3}$
12	457	836	$8.170\,692\,912\,027 \times 10^{-3}$	$8.170\,697\,771\,291 \times 10^{-3}$
13	548	1000	$8.170\,692\,965\,787 \times 10^{-3}$	$8.170\,695\,029\,079 \times 10^{-3}$
14	652	1173	$8.170\,692\,999\,658 \times 10^{-3}$	$8.170\,693\,953\,023 \times 10^{-3}$
15	763	1366	$8.170\,693\,014\,043 \times 10^{-3}$	$8.170\,693\,367\,924 \times 10^{-3}$
16	888	1566	$8.170\,693\,019\,245 \times 10^{-3}$	$8.170\,693\,193\,226 \times 10^{-3}$
Extrap.			$8.170\,693\,021\,30(21) \times 10^{-3}$	$8.170\,693\,117(8) \times 10^{-3}$

TABLE II. Extrapolated velocity (p) and length (r) two-photon decay rates $w^{(2\gamma)}/\alpha^6$ for various atoms and ions, including the heavy-helium cases with both electrons replaced by antiprotons ($\bar{\mathrm{p}}$), pions (π), or muons (μ). Units are atomic units. To convert to s^{-1}, multiply by α^6/τ_x where τ_e is given in Table I, $\tau_{\bar{\mathrm{p}}} = 1.317\,365\,60 \times 10^{-20}$ s, $\tau_\pi = 8.85610 \times 10^{-20}$ s, and $\tau_\mu = 1.169\,852\,69 \times 10^{-19}$ s for the antiprotonic, pionic, and muonic cases, respectively. Numbers in parentheses are estimated uncertainties.

Ion	Z	μ/M	$w_p^{(2\gamma)}/\alpha^6$	$w_r^{(2\gamma)}/\alpha^6$	$w_p^{(2\gamma)}/w_r^{(2\gamma)}$
$\bar{\mathrm{p}}^2$-^{4}He	2	$2.011\,020\,52 \times 10^{-1}$	$5.205\,617\,685\,79(17)\times10^{-3}$	$5.205\,617\,713\,1(13)\times10^{-3}$	0.999 999 9948(25)
π^2-^{4}He	2	$3.609\,30 \times10^{-2}$	$7.543\,045\,464\,90(31)\times10^{-3}$	$7.543\,045\,560(8)\times10^{-3}$	0.999 999 987(10)
μ^2-^{4}He	2	$2.756\,517\,98 \times 10^{-2}$	$7.686\,982\,264\,6(4)\times10^{-3}$	$7.686\,982\,309\,7(11)\times10^{-3}$	0.999 999 994(14)
^{3}He	2	$1.819\,212\,06 \times 10^{-4}$	$8.169\,874\,733\,147(22)\times10^{-3}$	$8.169\,874\,826(8)\times10^{-3}$	0.999 999 990(1)
^{4}He	2	$1.370\,745\,62 \times10^{-4}$	$8.170\,693\,021\,30(21)\times10^{-3}$	$8.170\,693\,117(8)\times10^{-3}$	0.999 999 988(9)
^{6}Li$^+$	3	$9.121\,675\,6 \times10^{-5}$	$3.109\,011\,875\,468(10)\times10^{-1}$	$3.109\,011\,8852(11)\times10^{-1}$	0.999 999 997(4)
^{7}Li$^+$	3	$7.820\,195\,0 \times10^{-5}$	$3.108\,946\,571\,280(10)\times10^{-1}$	$3.108\,946\,5812(11)\times10^{-1}$	0.999 999 997(4)
^{9}Be^{++}	4	$6.088\,199 \times10^{-5}$	$2.911\,617\,478\,8637(14)$	$2.911\,617\,4840(7)$	0.999 999 9982(25)
^{11}B^{3+}	5	$4.983\,870 \times10^{-5}$	$1.476\,948\,014\,809\,15(15)\times10^1$	$1.476\,948\,017\,98(15)\times10^1$	0.999 999 9978(10)
^{12}C^{4+}	6	$4.572\,544 \times10^{-5}$	$5.292\,996\,164\,0483(35)\times10^1$	$5.292\,996\,174\,30(21)\times10^1$	0.999 999 9981(4)
^{14}N^{5+}	7	$3.918\,481 \times10^{-5}$	$1.515\,442\,208\,159\,97(13)\times10^2$	$1.515\,442\,2110(6)\times10^2$	0.999 999 9981(4)
^{16}O^{6+}	8	$3.430\,541 \times10^{-5}$	$3.707\,994\,488\,493\,01(25)\times10^2$	$3.707\,994\,492\,78(16)\times10^2$	0.999 999 9988(4)
^{19}F^{7+}	9	$2.888\,173 \times 10^{-5}$	$8.077\,050\,937\,463\,53(4)\times10^2$	$8.077\,050\,9445(23)\times10^2$	0.999 999 999 12(29)
^{20}Ne^{8+}	10	$2.744\,620 \times 10^{-5}$	$1.608\,981\,338\,934\,41(5)\times10^3$	$1.608\,981\,339\,8859(33)\times10^3$	0.999 999 999 408(21)

TABLE III. Mass-polarization parameters C_x and D_x from Eq. (43) are shown for He and He-like ions, along with the accompanying algebraic relations, Eqs. (46) and (47).

Ion	C_p	C_r	$C_p - C_r$	D_p	D_r	$4C_p + D_p - D_r$
^{4}He	−5.2333588(30)	−1.23336(8)	−4.0000(8)	16.4344(10)	1.607(26)	−6.106(27)
^{7}Li$^+$	−5.385078(8)	−1.385078(12)	−4.000000(17)	17.124(27)	1.95(32)	−6.37(35)
^{9}Be^{++}	−5.487355(9)	−1.4871(5)	−4.0002(5)	17.799(7)	1.74(35)	−5.89(36)
^{11}B^{3+}	−5.557584(1)	−1.5575(1)	−4.00008(13)	18.3518(12)	2.09(12)	−5.97(12)
^{12}C^{4+}	−5.6094000(16)	−1.60943(13)	−3.99996(13)	18.8227(18)	2.47(14)	−6.08(14)
^{14}N^{5+}	−5.64973214(24)	−1.649718(24)	−4.000014(24)	19.24196(29)	2.661(28)	−6.018(28)
^{16}O^{6+}	−5.68233816(7)	−1.682327(12)	−4.000010(12)	19.61265(9)	2.903(16)	−6.020(16)
^{19}F^{7+}	−5.7094498(5)	−1.70942(6)	−4.000025(61)	19.9487(8)	3.099(99)	−5.99(10)
^{20}Ne^{8+}	−5.73247255(30)	−1.73249(3)	−3.99998(3)	20.2487(10)	3.40(10)	−6.08(10)

TABLE IV. Two-photon decay rates $w^{(2\gamma)}/\alpha^6$ for various atoms and ions, including the heavy-helium cases for both finite and infinite nuclear mass. Convert to s^{-1} by multiplying by α^6/τ_x, with τ values as given in Tables I and II.

Ion	Z	$w^{(2\gamma)}/\alpha^6$	$w_\infty^{(2\gamma)}/\alpha^6$	$w^{(2\gamma)}/w_\infty^{(2\gamma)}$
$\bar{p}^2$-^{4}He	2	5.205 617 685 79(17)$\times 10^{-3}$	8.173 194 7151(20)$\times 10^{-3}$	0.636 913 455 17(28)
π^2-^{4}He$^+$	2	7.543 045 464 90(31)$\times 10^{-3}$	8.173 194 7151(20)$\times 10^{-3}$	0.922 900 497 0(4)
μ^2-^{4}He	2	7.686 982 264 6(4)$\times 10^{-3}$	8.173 194 7151(20)$\times 10^{-3}$	0.940 511 334 0(5)
^{3}He	2	8.169 874 733 147(22)$\times 10^{-3}$	8.173 194 7151(20)$\times 10^{-3}$	0.999 593 796 30(36)
^{4}He	2	8.170 693 021 30(21)$\times 10^{-3}$	8.173 194 7151(20)$\times 10^{-3}$	0.999 693 914 82(35)
^{6}Li$^+$	3	3.109 011 875 468(10)$\times 10^{-1}$	3.108 554 078 983(7)$\times 10^{-1}$	1.000 147 269 91(4)
^{7}Li$^+$	3	3.108 946 571 280(10)$\times 10^{-1}$	3.108 554 078 983(7)$\times 10^{-1}$	1.000 126 262 01(4)
^{9}Be^{++}	4	2.911 617 478 8637(14)	2.910 640 612 6215(16)	1.000 335 618 983(8)
^{11}B^{3+}	5	1.476 948 014 809 15(15)$\times 10^1$	1.476 253 238 3922(19)$\times 10^1$	1.000 470 634 9825(16)
^{12}C^{4+}	6	5.292 996 164 0483(35)$\times 10^1$	5.289 756 826 1109(23)$\times 10^1$	1.000 612 379 367(7)
^{14}N^{5+}	7	1.515 442 208 159 97(13)$\times 10^2$	1.514 412 420 070 65(13)$\times 10^2$	1.000 679 991 8406(12)
^{16}O^{6+}	8	3.707 994 488 493 01(25)$\times 10^2$	3.705 284 196 490 4(9)$\times 10^2$	1.000 731 466 6998(24)
^{19}F^{7+}	9	8.077 050 937 463 53(4)$\times 10^2$	8.071 154 172 585 4(4)$\times 10^2$	1.000 730 597 4775(5)
^{20}Ne^{8+}	10	1.608 981 338 934 41(5)$\times 10^3$	1.607 689 583 705 86(3)$\times 10^3$	1.000 803 485 4745(4)

μ/M artificially set to $20(\mu/M)_{\rm actual}$. This then provided two equations in two unknowns to determine C_p and D_p from two independent values of the ratios $w_p^{(2\gamma)}/w_{p,\infty}^{(2\gamma)}$ for the velocity form, and similarly C_r and D_r from $w_r^{(2\gamma)}/w_{r,\infty}^{(2\gamma)}$ for the length form. The results are as shown in Table III. Since the results turned out to be less accurate for Ne^{8+}, we calculated the C and D coefficients by fitting the power series [Eq. (43)] to a range of values of μ/M between 10 and 100 times the nominal value for neon. Column 4 matches well the expected value of -4 for $C_{\rm p} - C_{\rm r}$ and column 7 confirms -6 for $4C_{\rm p} + D_{\rm p} - D_{\rm r}$, thus verifying that Eqs. (46) and (47) are correct. They also provide a sensitive test of the quality of the wave functions and pseudostates used. Once the C and D coefficients are known, they can be used to calculate the two-photon decay rate for any other isotope or value of μ/M since the remaining mass dependence in Eq. (43) can be trivially calculated.

In Table IV, successive columns list the name, atomic number Z, the rate $w^{(2\gamma)}$ for the system, the rate $w_\infty^{(2\gamma)}$ for the corresponding system with infinite nuclear mass, and the ratio $w^{(2\gamma)}/w_\infty^{(2\gamma)}$. The rates increase approximately as Z^6 while the ratio $w^{(2\gamma)}/w_0^{(2\gamma)}$ increases gradually, being less than unity for ^{4}He and a little larger than unity for the higher-Z nuclei. There is clearly a crossover point between $Z = 2$ and $Z = 3$ where the finite-nuclear-mass effects exactly cancel.

The spectral distribution as a function of energy is symmetric about the midpoint at $\hbar\omega = \frac{1}{2}(E_{\rm i} - E_{\rm f})$. In Table V we list the peak emission rate in s^{-1}, the energy difference in wave numbers, and the wavelength of the peak in nm units. Table II in Ref. [7] and Table V in Ref. [8] give the helium rates over half the spectrum, but exclude the factor of 1/2 due to double counting. Figure 1 shows the profile for ^{4}He, together with the difference curve between μ^2-^{4}He and ^{4}He(red), both normalized to unit integration rate. The difference curve across the middle shows that the effect of finite mass is to make the distribution curve higher and narrower for μ^2-^{4}He.

Table VI presents the final results for the two-photon decay rates, including an estimate of the relativistic correction $\Delta w_{\rm rel}^{(2\gamma)}$ [8]. The relativistic contribution becomes more

TABLE V. Maximum two-photon decay rates, energy ranges, and the wavelengths of the maximum rates. Values have converged to the figures quoted. Units are as stated in the table.

Ion	$w_{\rm max}$ (s^{-1})	$\Delta = \omega_{\rm i} - \omega_{\rm f}$ (cm^{-1})	Peak λ (nm)
$\bar{p}^2$-^{4}He	8.919 855 00 $\times 10^4$	2.984309 $\times 10^8$	6.701 720 $\times 10^{-2}$
π^2-^{4}He	1.8469 $\times 10^4$	4.5126 $\times 10^7$	4.4320 $\times 10^{-1}$
μ^2-^{4}He	1.421 736 $\times 10^4$	3.421 138 $\times 10^7$	5.846 008 $\times 10^{-1}$
^{3}He	7.255 592 87 $\times 10^1$	1.663 010 $\times 10^5$	1.202 639 $\times 10^2$
^{4}He	7.256 232 28 $\times 10^1$	1.663 025 $\times 10^5$	1.202 628 $\times 10^2$
^{6}Li$^+$	2.694 285 13 $\times 10^3$	4.914 063 $\times 10^5$	4.069 952 $\times 10^1$
^{7}Li$^+$	2.694 212 72 $\times 10^3$	4.914 072 $\times 10^5$	4.069 944 $\times 10^1$
^{9}Be^{++}	2.490 892 44 $\times 10^4$	9.811 005 $\times 10^5$	2.038 527 $\times 10^1$
^{11}B^{3+}	1.252 656 20 $\times 10^5$	1.635 617 $\times 10^6$	1.222 780 $\times 10^1$
^{12}C^{4+}	4.461 029 08 $\times 10^5$	2.454 648 $\times 10^6$	8.147 807
^{14}N^{5+}	1.271 097 75 $\times 10^6$	3.438 289 $\times 10^6$	5.816 846
^{16}O^{6+}	3.098 265 41 $\times 10^6$	4.586 539 $\times 10^6$	4.360 586
^{19}F^{7+}	6.727 920 98 $\times 10^6$	5.899 395 $\times 10^6$	3.390 178
^{20}Ne^{8+}	1.336 772 61 $\times 10^7$	7.376 858 $\times 10^6$	2.711 181

TABLE VI. Final values for the two-photon decay rates, including finite nuclear mass ($\Delta w^{(2\gamma)}_{\mu/M}$) and relativistic corrections ($\Delta w^{(2\gamma)}_{\rm rel}$) from Ref. [8]. The total $w^{(2\gamma)}_{\rm total}$ is compared with the relativistic CI calculations of Derevianko and Johnson [10]. Units are s^{-1} with an overall scale factor given in the last column for all the entries.

Ion	$w^{(2\gamma)}_{\infty}$	$\Delta w^{(2\gamma)}_{\mu/M}$	$\Delta w^{(2\gamma)}_{\rm rel}$	$w^{(2\gamma)}_{\rm total}$	Ref. [10]	Difference	Scale
$\bar{p}^2$-^{4}He	9.368 660 56(8)	−3.401 634 59(3)	−0.014(13)	5.953(13)			$\times 10^4$
π^2-^{4}He	1.393 610 183(13)	−0.107 446 652	−0.002 1(19)	1.284 1(19)			$\times 10^4$
μ^2-^{4}He	1.055 000 450(9)	−0.062 760 569	−0.001 6(15)	0.990 7(15)			$\times 10^4$
^{3}He	5.102 332 10(5)	−0.002 072 586	−0.008(7)	5.093(7)	5.102	−0.009(7)	$\times 10^1$
^{4}He	5.102 332 10(5)	−0.001 561 748	−0.008(7)	5.093(7)	5.102	−0.009(7)	$\times 10^1$
^{6}Li$^+$	1.940 596 769(17)	0.000 285 792	−0.002 0(17)	1.938 8(17)	1.940	−0.001 2(17)	$\times 10^3$
^{7}Li$^+$	1.940 596 769(17)	0.000 245 024	−0.002 0(17)	1.938 8(17)	1.940	−0.001 2(17)	$\times 10^3$
^{9}Be^{++}	1.817 044 074(16)	0.000 609 834	−0.002 2(16)	1.815 4(16)	1.816	−0.000 6(16)	$\times 10^4$
^{11}B^{3+}	9.215 899 72(8)	0.004 337 325	−0.014(8)	9.206(8)	9.211	−0.005(8)	$\times 10^4$
^{12}C^{4+}	3.302 270 041(30)	0.002 022 242	−0.006 3(33)	3.297 9(33)	3.300	−0.002 1(33)	$\times 10^5$
^{14}N^{5+}	9.454 118 46(9)	0.006 428 723	−0.023(10)	9.438(10)	9.444	−0.006(10)	$\times 10^5$
^{16}O^{6+}	2.313 121 264(21)	0.001 691 971	−0.006 8(29)	2.308 0(29)	2.310	−0.002 0(29)	$\times 10^6$
^{19}F^{7+}	5.038 630 60(5)	0.003 681 211	−0.018(6)	5.024(6)	5.029	−0.005(6)	$\times 10^6$
^{20}Ne^{8+}	1.003 642 572(9)	0.000 806 412	−0.004 4(14)	1.000 1(14)	1.001	−0.000 9(14)	$\times 10^7$

important with increasing Z and is larger in magnitude than the mass correction in all cases, but of opposite sign, except for $Z = 2$, where they both lower the infinite-nuclear-mass decay rate. For relativity we followed Ref. [8] assuming the effect for a two-electron system is bounded by the unscreened and fully screened shifts for a single-electron ion and applied the mean to the $w^{(2\gamma)}$ values. Our best estimates of the net rates are in the last column with the uncertainties indicated in parentheses representing the full single-electron range. Our final numbers are essentially the same as those of Derevianko and Johnson [10], who found this procedure in Ref. [8] for infinite-mass nuclei consistent with their relativistic calculations for the low-Z ions. However, for neutral helium, where relativistic effects are small and electron correlation effects are large, there is a marginal disagreement of 0.09 ± 0.07 s^{-1}.

Experimental lifetimes of $5.03(26) \times 10^{-4}$ s for both ^{4}He and ^{3}He [12] and $1.97(10) \times 10^{-2}$ s for ^{7}Li$^+$ [13] are entirely consistent with our respective calculations of $5.178(45) \times 10^{-4}$ and $1.9634(28) \times 10^{-2}$.

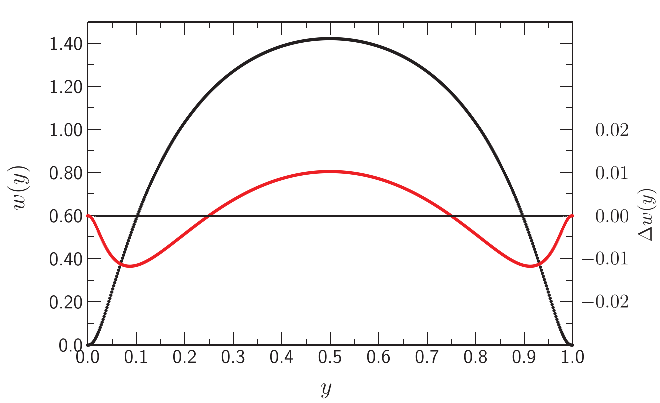

FIG. 1. Plots of the two-photon emission rate $w^{(2\gamma)}(^4\mathrm{He})$ and the difference $\Delta w^{(2\gamma)} = w^{(2\gamma)}(\mu^2\text{-}^4\mathrm{He}) - w^{(2\gamma)}(^4\mathrm{He})$ (red) as fractions y of the unit energy range normalized to unity.

V. ASTROPHYSICAL APPLICATION

Spitzer and Greenstein [36] investigated the two-photon emission by neutral hydrogen as a source of continuum radiation from planetary nebulae and Osterbrock [37] has further elaborated its importance where particle densities are less than about 10^4 cm^{-3}. Since hydrogen has its $2p\,^2P^o_{3/2}$ level very close to $2s\,^2S_{1/2}$, collisions can be competitive in depopulating that level to $1s\,^2S_{1/2}$. The hydrogen emission before mass and relativity corrections has an integrated rate of 8.2294 s^{-1} [5] extending from 121.9 μm to a maximum at 243.1 μm and then decreasing through the visible and infrared spectral regions. At low densities, this two-photon emission exceeds the contributions from the recombination of ionized hydrogen and helium from the Balmer limit at 364.6 μm to about 447.5 μm [37] if there is no significant recombination of twice-ionized helium.

For comparison, the two-photon spectrum of neutral helium has a total rate of 50.093 s^{-1} extending from 601.40 μm to a maximum at 120.28 μm deceasing to about 64% of the peak value at 364.6 μm. Typically, helium will be present with 1/10 the hydrogen abundance by number, so the two-photon emission by helium could be an important addition to the continuum emission around 400 μm in some planetary nebulae. Similarly for helium in the early universe, two-photon emission will affect the populations of the two lowest S states.

VI. CONCLUSIONS AND DISCUSSION

The results of this work improve the accuracy of the two-photon decay rates in helium and the heliumlike ions up to $Z = 10$ by several orders of magnitude from parts in 10^4 to parts in 10^9, at least in the nonrelativistic limit, and the effects of finite nuclear mass have been included to all orders in μ/M. The accuracy is sufficient to extract the leading two coefficients in the mass-polarization part of the finite-mass correction, and to test the algebraic relationships connecting the C_x and D_x coefficients. This provides a very sensitive way to test the equivalence of the L and V forms. It is interesting that all three contributions to the finite-mass effects must simultaneously be taken into account to bring the L and V forms into agreement. The results also demonstrate the high accuracy of our two-electron wave functions in doubled Hylleraas coordinates, and the pseudostates obtained from them to perform the sum over virtual transitions to intermediate P states.

The accuracy of the C_x and D_x coefficients could undoubtedly be improved by the use of perturbation theory for the mass-polarization operator $H_{\rm mp}$ in place of the simple finite-differencing method used here, but at substantially higher computational cost. Also, perturbation theory is of limited usefulness for the heavy-helium cases because μ/M is not sufficiently small, and so direct calculations with $H_{\rm mp}$ included explicitly in the Hamiltonian are essential. It would be much more useful and interesting to include relativistic effects as a perturbation, as has recently been done for the closely related tune-out wavelength [38], in order to improve the accuracy for ^{4}He and resolve an indicated discrepancy with the relativistic configuration-interaction (CI) calculations [10] shown in Table VI. Helium is the case of greatest astrophysical interest, and so an improved accuracy is important. Relativistic corrections will be the topic of a future publication.

ACKNOWLEDGMENTS

A.T.B. is grateful for financial support through the Natural Sciences and Engineering Research Council of Canada (NSERC) and Queen Elizabeth II graduate scholarships. Financial support by NSERC and by SHARCNET is gratefully acknowledged.

APPENDIX

The purpose of this Appendix is to give a simple way to sum over the two independent polarization vectors $\hat{\boldsymbol{\epsilon}}_1$ and $\hat{\boldsymbol{\epsilon}}_2$ perpendicular to $\mathbf{k}_1$ and $\mathbf{k}_2$ in order to obtain the angular correlation function $(1+\cos^2\theta_{12})$.

Let $\mathbf{k}_1$ and $\mathbf{k}_2$ define the xy plane (the collision plane). Then two possible independent choices for $|\hat{\boldsymbol{\epsilon}}_1\cdot\hat{\boldsymbol{\epsilon}}_2|^2$ are first, choose $\hat{\boldsymbol{\epsilon}}_1=\hat{\mathbf{e}}_z$, $\hat{\boldsymbol{\epsilon}}_2=\hat{\mathbf{e}}_z$ perpendicular to the xy plane. Then $|\hat{\boldsymbol{\epsilon}}_1\cdot\hat{\boldsymbol{\epsilon}}_2|^2=1$. Second, choose $\hat{\boldsymbol{\epsilon}}_1=\hat{\boldsymbol{k}}_1\times\hat{\mathbf{e}}_z$, $\hat{\boldsymbol{\epsilon}}_2=\hat{\boldsymbol{k}}_2\times\hat{\mathbf{e}}_z$ so that they both lie in the xy plane. Then, since by assumption $\hat{\boldsymbol{k}}_i\cdot\hat{\mathbf{e}}_z=\mathbf{0}$,

$$\begin{aligned}|\hat{\boldsymbol{\epsilon}}_1\cdot\hat{\boldsymbol{\epsilon}}_2|^2&=|(\hat{\boldsymbol{k}}_1\times\hat{\mathbf{e}}_z)\cdot(\hat{\boldsymbol{k}}_2\times\hat{\mathbf{e}}_z)|^2\\&=|\hat{\boldsymbol{k}}_1\cdot\hat{\boldsymbol{k}}_2|^2\\&=\cos^2\theta_{12}.\end{aligned}$$

The sum of both polarization contributions is thus a factor of $1+\cos^2\theta_{12}$.

Similarly for the case of single-photon transitions, we need to integrate $|\hat{\boldsymbol{\epsilon}}\cdot\mathbf{Q}|^2$ over solid angles $d\Omega$ for the direction of emission $\mathbf{k}$. For purposes of the integration, assume that $\mathbf{Q}$ points in the z direction. Then two possible independent choices for $\hat{\boldsymbol{\epsilon}}$ are first, choose $\hat{\boldsymbol{\epsilon}}_1$ to point in the $\hat{\mathbf{k}}\times\hat{\mathbf{Q}}$ direction. In this case, $\hat{\boldsymbol{\epsilon}}_1\cdot\mathbf{Q}=\mathbf{0}$, and so it does not contribute. Second, choose $\hat{\boldsymbol{\epsilon}}_2$ to lie in the $(\mathbf{k},\mathbf{Q})$ plane orthogonal to $\hat{\boldsymbol{\epsilon}}_1$. Then if $\hat{\mathbf{k}}\cdot\hat{\mathbf{e}}_z=\cos\theta$, $\hat{\boldsymbol{\epsilon}}_2\cdot\hat{\mathbf{e}}_z=\sin\theta$, and the angular integral is

$$\begin{aligned}\int_{4\pi}|\hat{\boldsymbol{\epsilon}}_2\cdot\mathbf{Q}|^2 d\Omega&=|\mathbf{Q}|^2\int_{4\pi}\sin^2\theta\, d\Omega\\&=\frac{8\pi}{3}|\mathbf{Q}|^2.\end{aligned}\tag{A1}$$

[1] M. Goeppert-Mayer, Ann. Phys. (Leipzig) **401**, 273 (1931).
[2] G. R. Blumenthal, G. W. F. Drake, and W. P. Tucker, Strophys. J. **172**, 205 (1972).
[3] Ya. B. Zel'dovich, V. G. Kurt, and R. A. Sunyaev, Zh. Eskp. Teor. Fiz. **55**, 278 (1968) [Sov. Phys. JETP Lett. **28**, 146 (1969)].
[4] P. J. E. Peebles, Astrophys. J. **153**, 1 (1968).
[5] G. Breit and E. Teller, Astrophys. J. **91**, 215 (1940).
[6] A. Dalgarno, Mon. Not. R. Astron. Soc. **131**, 311 (1966).
[7] G. W. F. Drake, G. A. Victor, and A. Dalgarno, Phys. Rev. **180**, 25 (1969).
[8] G. W. F. Drake, Phys. Rev. A **34**, 2871 (1986).
[9] S. P. Goldman and G. W. F. Drake, Phys. Rev. A **24**, 183 (1981).
[10] A. Derevianko and W. R. Johnson, Phys. Rev. A **56**, 1288 (1997).
[11] O. Bely and P. Faucher, Astron. Astrophys. **1**, 37 (1969).
[12] R. S. Van Dyck, Jr., C. E. Johnson, and H. A. Shugart, Phys. Rev. A **4**, 1327 (1971).
[13] M. H. Prior and H. A. Shugart, Phys. Rev. Lett. **27**, 902 (1971).
[14] H. Gould and R. Marrus, Phys. Rev. A **28**, 2001 (1983).
[15] R. W. Dunford, H. G. Berry, K. O. Groeneveld, M. Hass, E. Bakke, M. L. A. Raphaelian, A. E. Livingston, and L. J. Curtis, Phys. Rev. A **38**, 5423 (1988).
[16] R. W. Dunford, H. G. Berry, S. Cheng, E. P. Kanter, C. Kurtz, B. J. Zabransky, A. E. Livingston, and L. J. Curtis, Phys. Rev. A **48**, 1929 (1993).
[17] R. Marrus, V. San Vicente, P. Charles, J. P. Briand, F. Bosch, D. Liesen, and I. Varga, Phys. Rev. Lett. **56**, 1683 (1986).
[18] A. Simionovici, B. B. Birkett, J. P. Briand, P. Charles, D. D. Dietrich, K. Finlayson, P. Indelicato, D. Liesen, and R. Marrus, Phys. Rev. A **48**, 1695 (1993).
[19] P. H. Mokler and R. W. Dunford, Phys. Scr. **69**, C1 (2004).
[20] A. V. Volotka, A. Surzhykov, V. M. Shabaev, and G. Plunien, Phys. Rev. A **83**, 062508 (2011).
[21] D. Banas, A. Gumberidze, S. Trotsenko, A. V. Volotka, A. Surzhykov, H. F. Beyer, F. Bosch, A. Brauning-Demian, S. Fritzsche, S. Hagmann, C. Kozhuharov, A. Kumar, X. Ma, R. Mann, P. H. Mokler, D. Sierpowski, U. Spillmann, S. Tashenov, Z. Stachura, A. Warczak, and T. Stohlker, Phys. Rev. A **87**, 062510 (2013).
[22] L. Safari, P. Amaro, J. P. Santos, and F. Fratini, Phys. Rev. A **90**, 014502 (2014).
[23] T. A. Zalialiutdinov, D. A. Solovyev, L. N. Labzowsky, and G. Plunien, Phys. Rep. **737**, 1 (2018).
[24] G. Barton and A. Calogeracos, J. Opt. B: Quantum Semiclass. Opt. **7**, S21 (2005).
[25] C. K. Au, Phys. Lett. A **232**, 162 (1997).

[26] P. J. Mohr, D. B. Newell, and B. N. Taylor, Rev. Mod. Phys. **88**, 035009 (2016).
[27] Z. Fried and A. D. Martin, Nuovo Cimento **29**, 574 (1963).
[28] Z.-C. Yan and G. W. F. Drake, Phys. Rev. A **52**, R4316(R) (1995).
[29] G. W. F. Drake and D. C. Morton, Astrophys. J. Suppl. **170**, 251 (2007).
[30] H. A. Bethe and E. E. Salpeter *Quantum Mechanics of One- and Two-Electron Atoms* (Springer, Berlin, 1957), Eq. (59.11).
[31] A. I. Akhiezer and V. B. Berestetskii, *Quantum Electrodynamics* (Wiley Interscience, New York, 1965), p. 490.
[32] G. W. F. Drake, Phys. Scr. **1999**, 83 (1999).
[33] G. W. F. Drake and A. J. Makowski, J. Opt. Soc. Am. B **5** (1988).
[34] G. W. F. Drake and Z.-C. Yan, Phys. Rev. A **46**, 2378 (1992).
[35] D. C. Morton, E. E. Schulhoff, and G. W. F. Drake, J. Phys. B **48**, 235001 (2015).
[36] L. Spitzer, Jr. and J. L. Greenstein, Astrophys. J. **114**, 407 (1951).
[37] D. E. Osterbrock, *Astrophysics of Gaseous Nebulae* (W. H. Freeman, San Francisco, 1974).
[38] G. W. F. Drake, J. G. Manalo, P.-P. Zhang, and K. G. H. Baldwin, Hyperfine Interact. **240**, 31 (2019).